MEDICAL SCIENCE MONITOR

Rosmarinic Acid Combined with Adriamycin Induces Apoptosis by Triggering Mitochondria-Mediated Signaling Pathway in HepG2 and Bel-7402 Cells

Authors' Contribution:
Study Design A
Data Collection B
Statistical Analysis C
Data Interpretation D
Manuscript Preparation E
Literature Search F
Funds Collection G

ABCDEFG 1 Youxia Huang*
BCDEF 2 Yingjian Cai*
BCDF 3 Ronggui Huang
BCDF 3 Xingzhong Zheng

1 Department of Pharmacology, Quanzhou Medical College, Quanzhou, Fujian, P.R. China
2 Department of Pediatrics, Fujian Medical University 2nd Clinical Medical College, Quanzhou, Fujian, P.R. China
3 Department of Nephrology, Fujian Medical University 2nd Clinical Medical College, Quanzhou, Fujian, P.R. China

Corresponding Author:
Source of support:

* These 2 authors contributed equally to this study
Youxia Huang, e-mail: hyx15959880099@hainan.net
This study was funded by the Quanzhou City Science and Technology Project (grant no. 2012Z75) and the Science and Technology Project of the Education Department of Fujian Province (grant no. JA12433)

Background: Hepatic carcinoma is the third leading cause of cancer-related deaths. This study aimed to evaluate the anti-tumor effects of rosmarinic acid (RosA) combined with Adriamycin (ADM) on proliferation and apoptosis of hepatic carcinoma cell lines.

Material/Methods: Human HepG2 and Bel-7402 cells were treated with RosA and ADM and divided into HepG2 or Bel-7402, 25 μg/ml, 50 μg/m, and 100 μg/ml RosA+0.4 μg/ml ADM groups, respectively. The Cell Counting Kit-8 (CCK-8) assay was used to evaluate cell viability. Immunohistochemistry assay was used to examine B cell lymphoma-2 (Bcl-2) and Bcl-2-associated X (Bax) expression. Cell cycle analysis was used to detect cell cycle distribution. Flow cytometry and terminal deoxynucleotidyl transferase-mediated d-UTP nick-end labeling (TUNEL) assay were utilized to evaluate apoptosis.

Results: RosA combined with ADM damaged cell morphology and decreased cell viability, and significantly decreased S-phase cell numbers compared to the HepG2 or Bel-7402 group ($p<0.05$). Apoptosis rates in the RosA combined with ADM group were significantly increased compared to the HepG2 or Bel-7402 group ($p<0.05$). TUNEL assay showed that RosA combined with ADM significantly induced DNA damage (TUNEL-positive staining) in the HepG2 and Bel-7402 groups ($p<0.05$). RosA combined with ADM significantly reduced Bcl-2 expression in HepG2 or Bel-7402 cells ($p<0.05$). RosA combined with ADM significantly increased Bax expression in HepG2 and Bel-7402 cells ($p<0.05$). Cell viability, apoptosis, cell cycle, and Bcl-2 and Bax expression were changed with increased concentrations of RosA.

Conclusions: RosA combined with ADM damaged tumor cell morphologies, decreased cell viability, and induced apoptosis of HepG2 and Bel-7402 by triggering the mitochondria-mediated signaling pathway.

MeSH Keywords: Apoptosis • Liver Neoplasms • Medicine, Chinese Traditional

Full-text PDF: https://www.medscimonit.com/abstract/index/idArt/910673

📄 2619   ▦ —   📊 8   📖 27

Background

Hepatic carcinoma is the third leading cause of cancer-related deaths [1,2]. Of the total worldwide incidence of hepatic carcinoma, China accounts for 55%, and the mortality caused by hepatic carcinoma is second only to that of lung cancer [3,4]. Hepatocellular cancer is the most common type of hepatic carcinoma in adults [5]. The high mortality of hepatic carcinoma is also associated with the recurrence of hepatocellular cancer. Clinically, patients are usually diagnosed with hepatic carcinoma at advanced stages, so it is urgent to selecting the effective treatment methods such as chemotherapy [6]. Nowadays, the most commonly used single-agent drugs for hepatic carcinoma therapy include cisplatin, sorafenib, doxorubicin, and 5-fluorouracil [7]. However, these drugs exhibit low selectivity and always induced serious adverse effects clinically. Therefore, it is urgent to develop new drugs that exhibit higher selectivity, higher efficacy, and fewer adverse effects.

Combination therapy has emerged as a novel strategy for treating hepatic carcinoma and shows fewer adverse effects and better long-term efficacy [8]. The most commonly used combination therapies are the combination of chemotherapy with chemo-sensitizers and the combination of anti-cancer agents targeting multiple pathways, both of which can reduce adverse effects and maximize therapeutic effects [9,10].

Rosmarinic acid (RosA) is a natural compound with several biological activities, such as anti-inflammatory, anti-angiogenic, anti-oxidant, anti-fibrosis, and hepato-protective functions [11]. RosA is extracted from medicinal species of *Lamiaceae* and *Boraginaceae* [12]. Recent studies reported that RosA has anti-tumor activity in gastric cancer [13], leukemia [14], and colon cancer [15] by triggering signaling pathways. Although these biological activities have been clearly defined, the effects of RosA in hepatic carcinoma have not been fully clarified. Adriamycin (ADM) is an anthracycline antibiotic and is considered as the most efficient drug for treating hepatic carcinoma [8,16]. ADM is broad-spectrum anti-tumor drug that can cause tumor cells apoptosis by regulating transcription [17]. However, ADM can only target the proliferating-stage tumor cells and reduce tumor volume, inducing complete remission. Therefore, we combined RosA with ADM in this study and evaluated the anti-tumor effects on apoptosis of hepatic carcinoma cell lines HepG2 and Bel-7402.

Material and Methods

Cell culture

The human hepatoma cell lines HepG2 and Bel-7402 were purchased from the Type Culture Collection of Shanghai Academy of Science (Shanghai, China). HepG2 and Bel-7402 cells were cultured in Roswell Park Memorial Institute 1640 (PRMI 1640, Gibco BRL. Co., Ltd., Grand Island, NY, USA) supplemented with heat-inactivated fetal bovine serum (FBS, 100 ml/l, Gibco BRL. Co., Ltd.), 100 U/ml penicillin (Beyotime Biotech, Shanghai, China) and 100 U/ml streptomycin (Beyotime Biotech). Both cell lines were seeded in 6-well plates (Corning, NY, USA) and grown in a humidified atmosphere containing 5% CO_2 at 37°C. This study was approved by the Ethics Committee of Quanzhou Medical College, Quanzhou, China.

Cell treatment and trial grouping

The cell suspensions were adjusted to the concentration of 10^5–10^6 cells/well. According to the pre-experiment results, the optimal dosage of ADM was 0.4 µg/ml and the concentration of RosA ranging from 25 µg/ml to 100 µg/ml had the best effects on cell viability (Supplementary Figure 1). Therefore, HepG2 and Bel-7402 cells were incubated with ADM (Beijing Huafeng United Tech. Co., Ltd., Beijing, China) at a final concentration of 0.4 µg/ml and RosA (Aladdin Reagent Co., Ltd., Shanghai, China) at the final concentration of 25 µg/ml, 50 µg/ml, and 100 µg/ml, respectively. HepG2 cells were divided into HepG2 group, HepG2+25 µg/ml RosA+0.4 µg/ml ADM group, HepG2+50 µg/ml RosA+0.4 µg/ml ADM group, and HepG2+100 µg/ml RosA+0.4 µg/ml ADM group. The Bel-7402 cells were divided into Bel-7402 group, Bel-7402+25 µg/ml RosA+0.4 µg/ml ADM group, Bel-7402+50 µg/ml RosA+0.4 µg/ml ADM group, and Bel-7402+100 µg/ml RosA+0.4 µg/ml ADM group.

Cell counting kit-8 (CCK-8) assay

The cell viabilities of HepG2 and Bel-7402 cells were evaluated by using CCK-8 assay kits (Beyotime Biotech., Shanghai, China) according to the manufacturer's instruction. The exponentially growing H-ILCSCs, HCCLM3, and HL-7702 cells (5×10⁴ cells/ml) were seeded into a 96-well plate (Corning Costar, Acton, MA, USA) and incubated for 72 h. At 24 h, 36 h, and 48 h, the CCK-8 solution (10 µl/ml medium) was added to 3 randomly selected wells and incubated at 37°C for 4 h. The cell viability was represented by optimal density (OD) values detected at 450 nm with an ELISA reader (Mode: Elx800, Bio-Tek Inc., Winooski, VT, USA).

Immunohistochemistry assay

The HepG2 and Bel-7402 cells were fixed with 4% paraformaldehyde (Sangon Biotech., Shanghai, China) for 15 min, then washed in phosphate-buffered saline (PBS). Endogenous peroxidase was inactivated by using 3% hydrogen peroxide (Beyotime Biotech, Shanghai, China) at room temperature for 5 min. Then, the cells were blocked using 5% bovine serum albumin (BSA, Gibco BRL. Co., Ltd., Grand Island, New York, USA) for 20 min
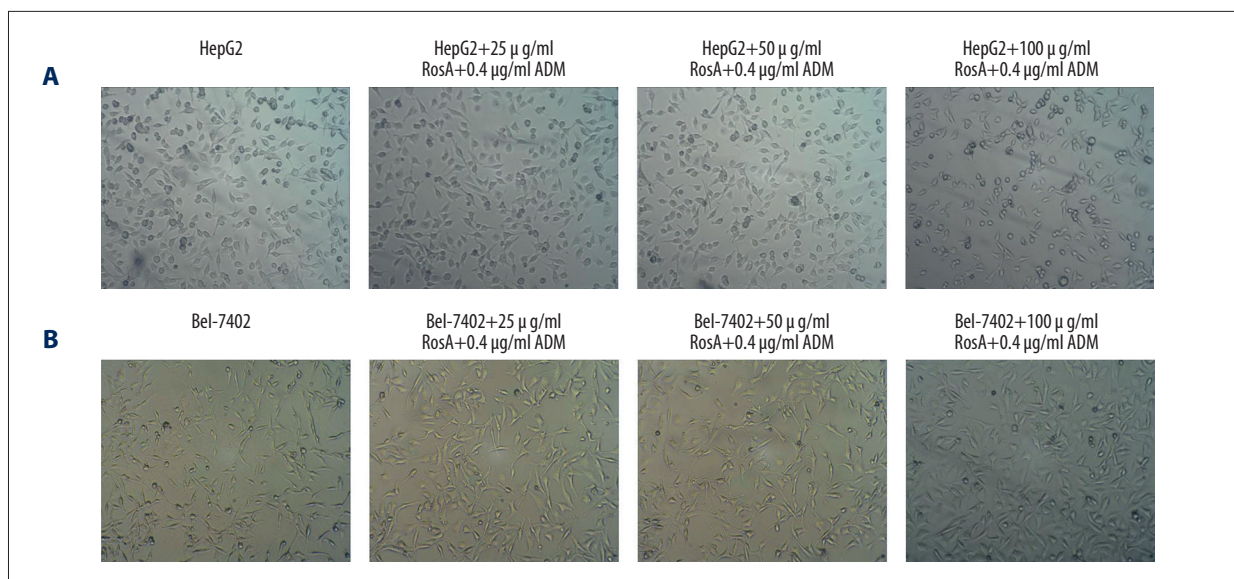
Figure 1. Morphology of HepG2 and Bel-7402 cells. (**A**) HepG2 cell morphology images. (**B**) Bel-7402 cell morphology images. In of HepG2 and Bel-7402 cells, untreated cells exhibited integrated morphology and many living cells, and treated cells exhibited morphology of cell fragmentation and more dead cells.

and washed with PBS. The cells were incubated with mouse anti-human B cell lymphoma-2 (Bcl-2) monoclonal antibody (1: 3000, cat. no. AE483629, RD Systems, Minneapolis, MN, USA) and mouse anti-human Bcl-2-associated X protein (Bax) monoclonal antibody (1: 3000, cat. no. 610983, RD Systems, Minneapolis, MN, USA) at 4°C overnight. Then, the tumor tissues were incubated with Biotin-conjugated rabbit anti-mouse IgG (1: 1000, cat. no.176-003, RD Systems, Minneapolis, MN, USA) at room temperature for 1 h. Finally, images of stained cells were captured by using an inverted fluorescence microscope (Mode: CKX 41, Olympus, Japan).

Cell cycle analysis

The cell cycle distribution of HepG2 and Bel-7402 cells was evaluated with the Cell Cycle and Apoptosis Analysis kit (BD Biosciences, San Jose, CA, USA) following the manufacturer's instruction. Briefly, HepG2 and Bel-7402 cells were harvested 24 h after the different treatments, washed 3 times using PBS, and fixed at 4°C for 1 h using 70% ethanol. Then, the HepG2 and Bel-7402 cells were stained using a propidium iodide (PI) solution containing RNase at 4°C for 30 min. Finally, about 20 000 cells were analyzed with the FACS Vantage SE flow cytometer (BD Biosciences, San Jose, CA, USA). The cell cycle distribution of HepG2 and Bel-7402 cells was analyzed using ModFIT cell cycle analysis software (Version 2.01.2; BD Biosciences, San Jose, CA, USA).

Flow cytometry assay

The apoptosis of HepG2 and Bel-7402 cells was evaluated with flow cytometry and an Annexin V-FITC apoptosis kit (BD Biosciences, San Jose, CA, USA). In brief, HepG2 and Bel-7402 cells were harvested and re-suspended in the Annexin V binding buffer (BD Biosciences) and incubated with Annexin V-PE and PI (BD Biosciences) for 15 min in the dark at room temperature. Then, the cells were analyzed using a FACS Vantage SE flow cytometer (BD Biosciences, San Jose, CA, USA). Finally, fluorescence was measured by using a 530/578 band filter to monitor Annexin V binding and using a 546/647 band filter to monitor PI uptake in HepG2 and Bel-7402 cells.

Terminal deoxynucleotidyl transferase-mediated d-UTP nick-end labeling (TUNEL) assay

The TUNEL assay was conducted by using the In Situ Cell Death Detection kit-POD (Roche Diagnostics, Indianapolis, IN, USA) according to the manufacturer's instructions. Briefly, the HepG2 and Bel-7402 cells were washed with PBS and centrifuged. The obtained supernatant was discarded, and the pellets were re-suspended in the DNA labeling solution (50 µl, Beyotime Biotech, Shanghai, China) and incubated at 37°C for 2 h. Then, the detailed processes for the TUNEL were conducted according to a previous report [18]. Finally, the cells were imaged using an inverted microscope (Mode: IX70, Olympus, Japan) and analyzed using an Olympus camera system (Mode: BH-2, Olympus, Japan).

Statistical analysis

Data in this study are described as mean ± standard deviation (SD) and were analyzed using SPSS software 20.0 (SPSS, Inc., Chicago, IL, USA). The data were obtained from at least 3
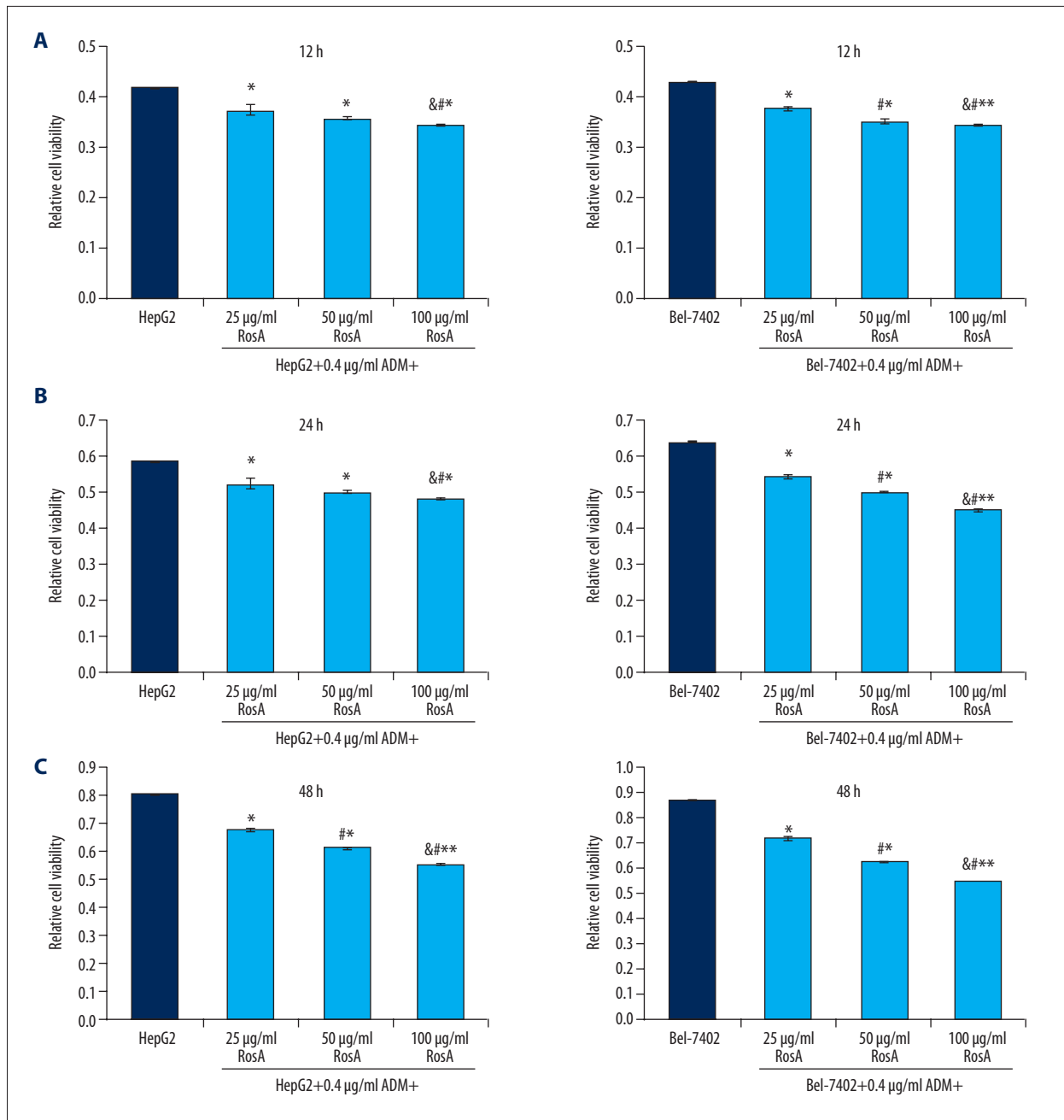
Figure 2. Cell viabilities for HepG2 and Bel-7402 cells undergoing RosA and ADM treatment at 12 h, 24 h, and 48 h. (**A**) Cell viabilities of HepG2 and Bel-7402 cells at 12 h. (**B**) Cell viabilities of HepG2 and Bel-7402 cells at 24 h. (**C**) Cell viabilities of HepG2 and Bel-7402 cells at 48 h. ** $p<0.01$, * $p<0.05$ *vs.* HepG2 or Bel-7402 group, # $p<0.01$ *vs.* 25 µg/ml RosA+0.4 µg/ml ADM group, & $p<0.01$ *vs.* 50 µg/ml RosA+0.4 µg/ml ADM group.

independent experiments. The *t* test was used for statistical analysis between 2 group and one-way ANOVA was used for statistical analysis of multiple groups. A statistical significance was defined when $p<0.05$.

Results

RosA combined with ADM damaged cell morphology of HepG2 and Bel-7402 cells

To evaluate the effects of the RosA combined with ADM strategy on HepG2 and Bel-7402 cell growth, were observed
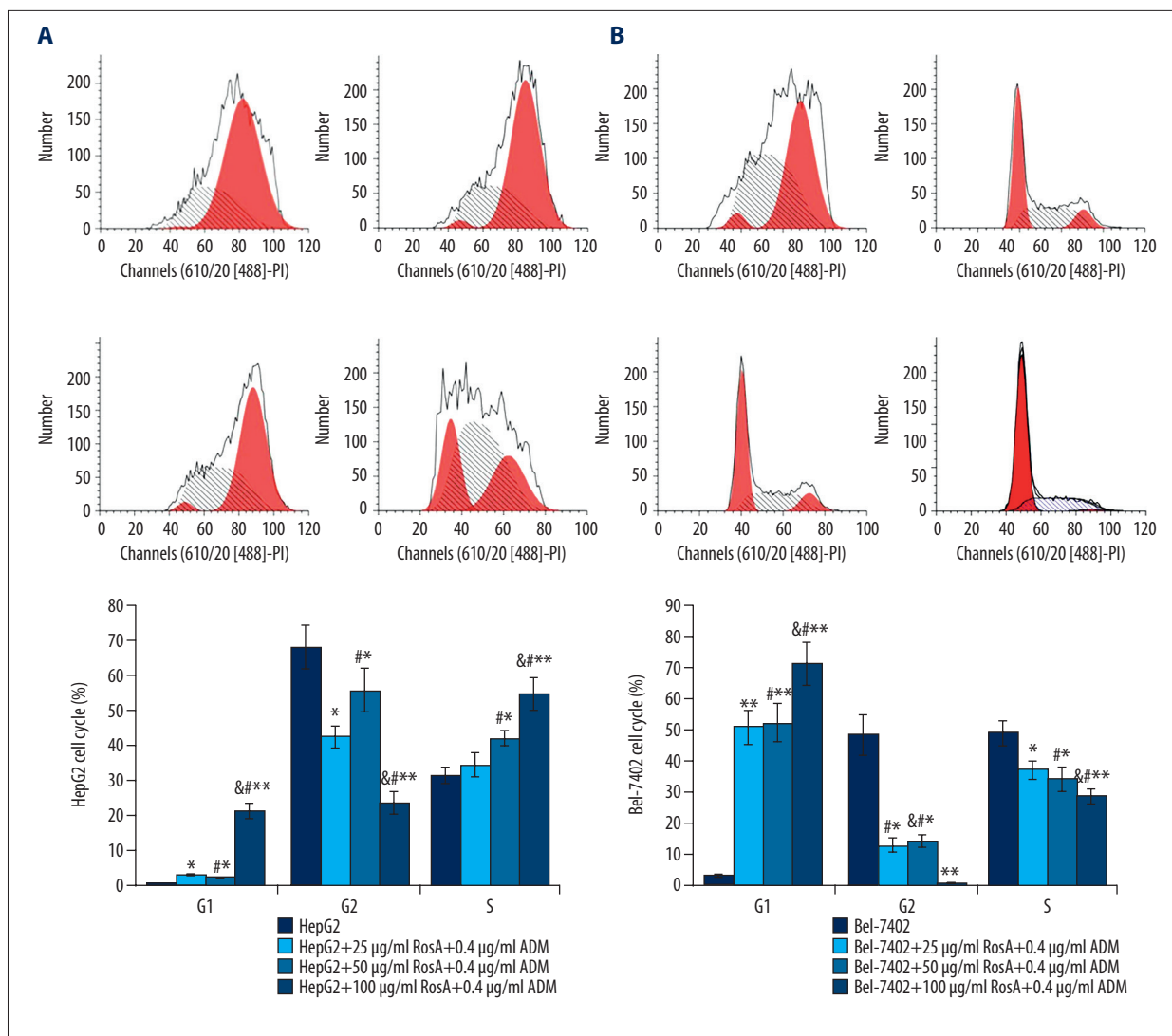
Figure 3. Cell cycle analysis for HepG2 and Bel-7402 cells. (**A**) Flow cytometry images and statistical analysis for cell cycle of HepG2 cells. (**B**) Flow cytometry images and statistical analysis for cell cycle of Bel-7402 cells. ** $p<0.01$, * $p<0.05$ *vs.* HepG2 or Bel-7402 group, # $p<0.01$ *vs.* 25 µg/ml RosA+0.4 µg/ml ADM group, & $p<0.01$ *vs.* 50 µg/ml RosA+0.4 µg/ml ADM group.

the morphologies. The HepG2 and Bel-7402 cells untreated with RosA and ADM exhibited integrated morphology and many living cells (Figure 1). However, the cells treated with RosA combined with ADM exhibited morphology of cell fragmentation and more dead cells (Figure 1). Therefore, the results indicated that, compared with the HepG2 (Figure 1A) group and the Bel-7402 group (Figure 1B) group, the RosA combined with ADM treatment group had obviously damaged cell morphologies.

RosA combined with ADM decreased cell viability of HepG2 and Bel-7402 cells

Due to the damaged cell morphologies induced by RosA and ADM treatment, the cell viabilities of HepG2 and Bel-7402 cells were evaluated using CCK-8 assay. The results showed that for

HepG2 and Bel-7402 cells, the cell viabilities of different concentrations of RosA combined with ADM were significantly decreased compared to the HepG2 group and the Bel-7402 group at 12 h (Figure 2A), 24 h (Figure 2B), and 48 h (Figure 2C) (all $p<0.05$). Cell viabilities decreased with increased RosA concentrations (Figure 2, $p<0.05$), which illustrates the dose-dependent differences among different treatment groups.

RosA combined with ADM regulated the proportions of cell cycle

To support the proliferation-inhibitive effects of RosA combined with ADM, the proportions of cells in each phase were analyzed (Figure 3). The results showed that the RosA combined with ADM treatment group had a significantly decreased G2
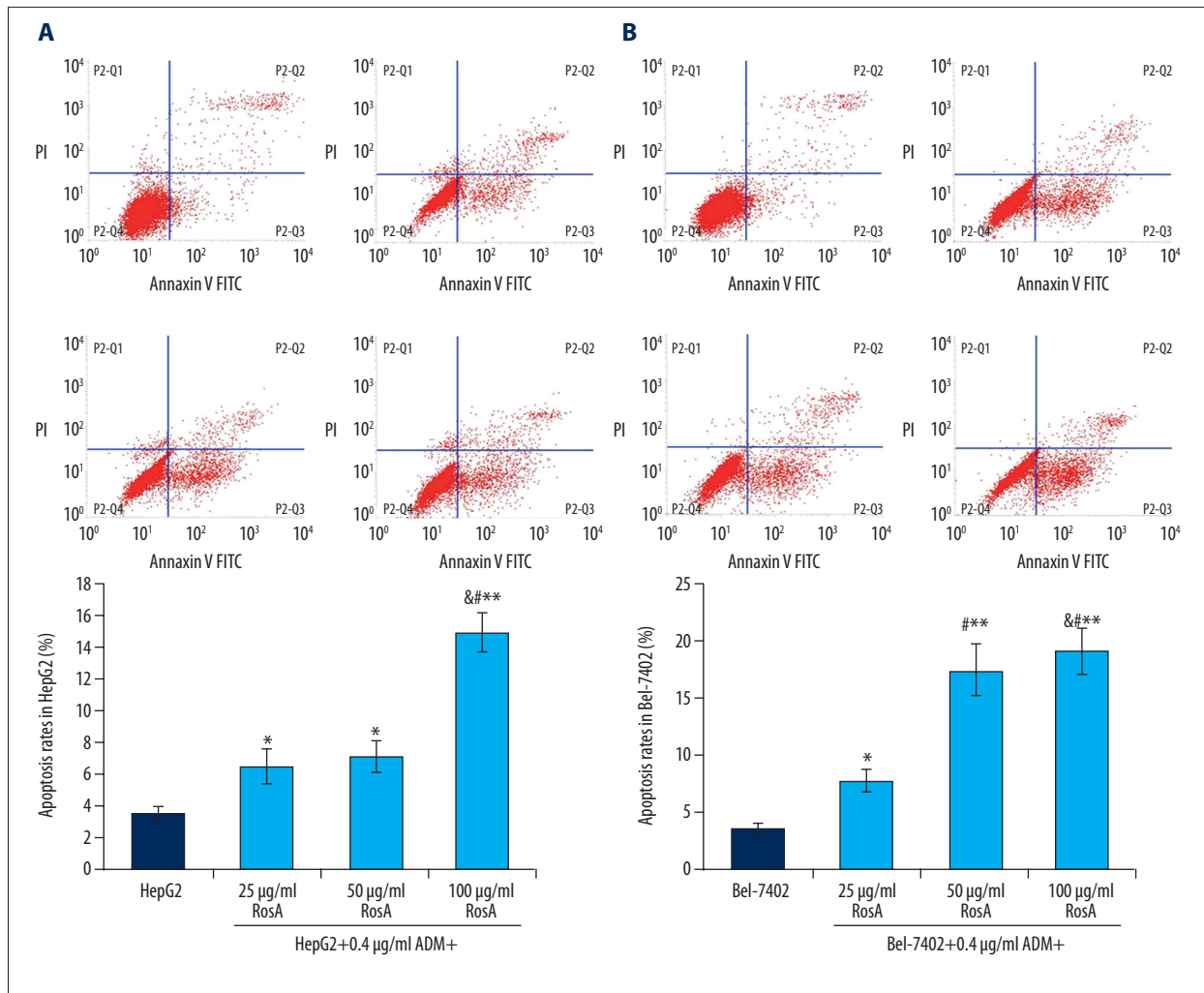
Figure 4. Cell apoptosis analysis of HepG2 and Bel-7402 cells using flow cytometry assay. (**A**) Flow cytometry images and statistical analysis for apoptosis of HepG2 cells. (**B**) Flow cytometry images and statistical analysis for apoptosis of Bel-7402 cells. ** $p<0.01$, * $p<0.05$ *vs.* HepG2 or Bel-7402 group, # $p<0.01$ *vs.* 25 µg/ml RosA+0.4 µg/ml ADM group, & $p<0.01$ *vs.* 50 µg/ml RosA+0.4 µg/ml ADM group.

phase proportion and an increased G1 phase proportion compared to the HepG2 and Bel-7402 groups (Figure 3A, $p<0.05$). RosA combined with ADM significantly decreased the proportion of cells in S-phase in Bel-7402 cells but increased the proportion of S-phase cells in the HepG2 group (Figure 3B, $p<0.05$). The number of cells in S-phase was significantly increased with increased RosA concentrations (Figure 3, $p<0.05$), which illustrated the dose-dependent discrepancy of S-phase cells among different treatment groups.

RosA combined with ADM triggered apoptosis of HepG2 and Bel-7402 cells

Flow cytometry assay was used to evaluate the apoptosis of HepG2 and Bel-7402 cells undergoing RosA and ADM treatment (Figure 4). The results showed that the apoptosis rates in

the RosA (different concentrations) combined with ADM group were significantly increased compared to the HepG2 group (Figure 4A, $p<0.05$). Apoptosis rates were also significantly increased in the RosA (different concentrations) combined with ADM group compared to the Bel-7402 group (Figure 4B, $p<0.05$). For HepG2 and Bel-7402 cells, the apoptosis rates increased with increased RosA concentrations (Figure 4, $p<0.05$), which illustrates the dose-dependent difference in apoptosis among different treatment groups.

RosA combined with ADM induced DNA damage of HepG2 and Bel-7402 cells

To confirm that RosA and ADM caused apoptosis, the DNA damage in HepG2 (Figure 5A) and Bel-7402 (Figure 5B) cells was also examined using TUNEL assay. The results indicated that the numbers
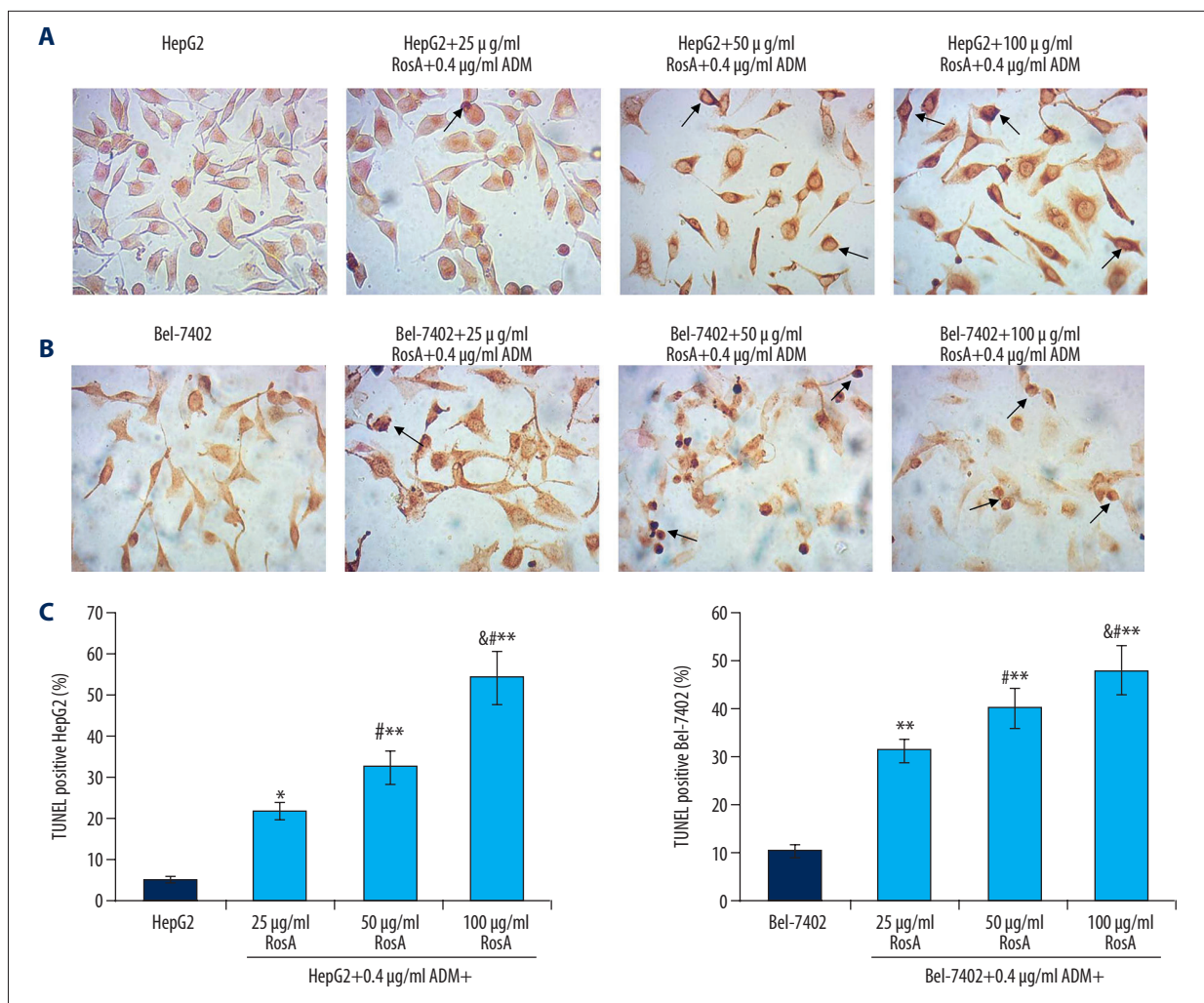
This work is licensed under Creative Common Attribution-
NonCommercial-NoDerivatives 4.0 International (CC BY-NC-ND 4.0)

7903

Indexed in: [Current Contents/Clinical Medicine] [SCI Expanded] [ISI Alerting System]
[ISI Journals Master List] [Index Medicus/MEDLINE] [EMBASE/Excerpta Medica]
[Chemical Abstracts/CAS]

Figure 5. TUNEL staining of damaged DNA in HepG2 and Bel-7402 cells. (**A**) TUNEL staining of HepG2 cells. (**B**) TUNEL staining of Bel-7402 cells. (**C**) Statistical analysis of TUNEL staining-positive cells. Black arrows represent the TUNEL staining-positive cells. ** $p<0.01$, * $p<0.05$ *vs.* HepG2 or Bel-7402 group, # $p<0.01$ *vs.* 25 μg/ml RosA+0.4 μg/ml ADM group, & $p<0.01$ *vs.* 50 μg/ml RosA+0.4 μg/ml ADM group.

of TUNEL-positive HepG2 cells (damaged DNA) were significantly increased in the HepG2+25/50/100 μg/ml RosA+0.4 μg/ml ADM group compared to the HepG2 group (Figure 5C, all $p<0.05$). Meanwhile, the TUNEL-positive Bel-7402 cell (damaged DNA) numbers were significantly higher in the Bel-7402+25/50/100 μg/ml RosA+0.4 μg/ml ADM group compared to the Bel-7402 group (Figure 5C, all $p<0.05$). Moreover, the numbers of TUNEL-positive cells increased with increased concentration of RosA (Figure 5, $p<0.05$), which illustrates the dose-dependent difference in DNA damage among different treatment groups.

RosA combined with ADM reduced Bcl-2 expression in HepG2 and Bel-7402 cells

The mitochondria-associated signaling pathway key bio-marker, Bcl-2, was examined in both HepG2 (Figure 6A)

and Bel-7402 (Figure 6B) cells by using immunohisto-chemistry assay. The results indicated that expression of Bcl-2 in HepG2 cells were significantly decreased in the HepG2+25/50/100 μg/ml RosA+0.4 μg/ml ADM group compared to the HepG2 group (Figure 6C, all $p<0.05$). Meanwhile, expression of Bcl-2 in Bel-7402 cells was significantly reduced in the Bel-7402+25/50/100 μg/ml RosA+0.4 μg/ml ADM group compared to the Bel-7402 group (Figure 6C, all $p<0.05$). Moreover, the expressions of Bcl-2 decreased with increased concentration of RosA (Figure 6, $p<0.05$), which illustrates the dose-dependent difference in Bcl-2 expression among different treatment groups.
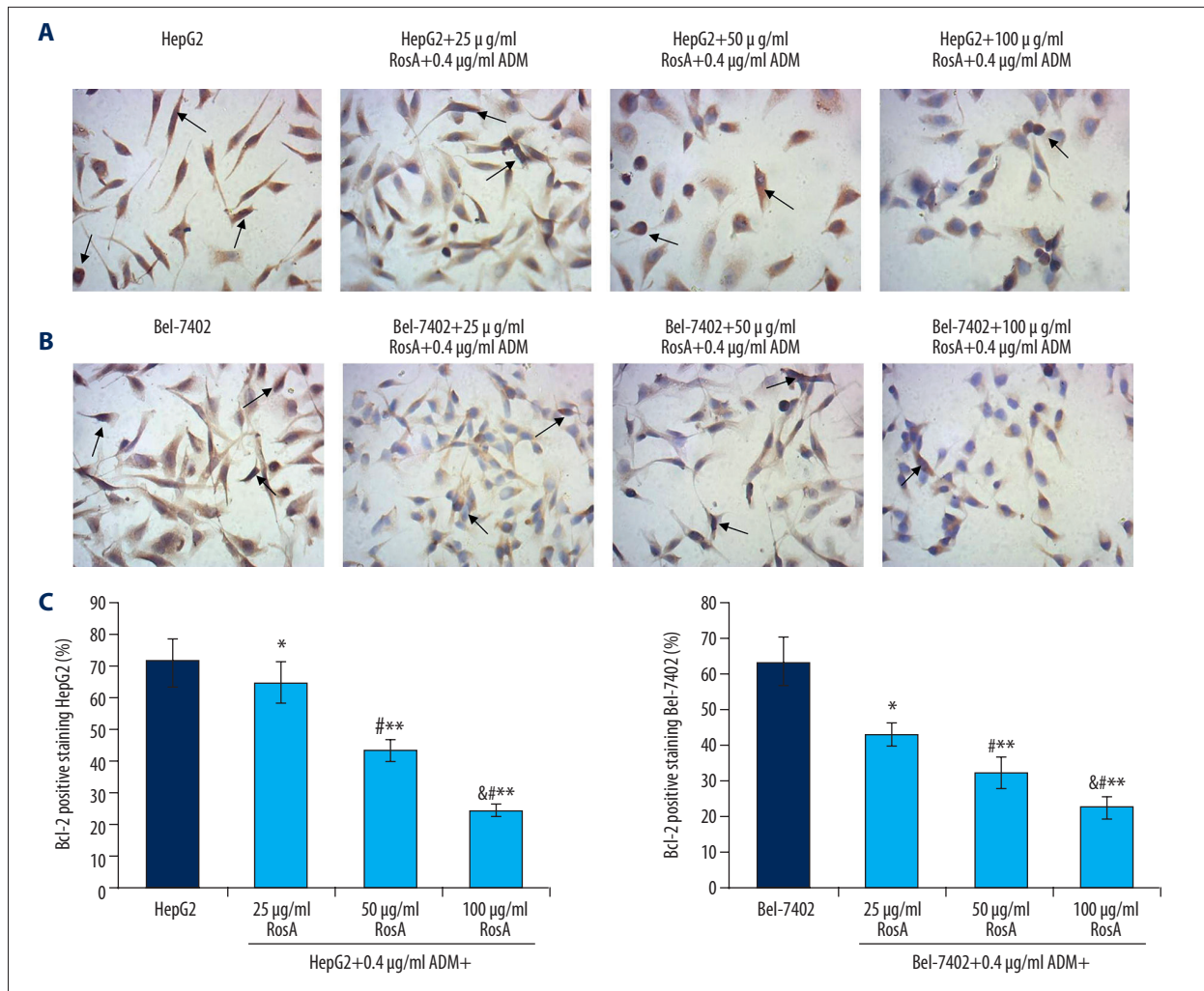
Figure 6. Evaluation for the Bcl-2 expression in HepG2 and Bel-7402 cells by immunohistochemistry assay. (**A**) Images of Bcl-2-positive HepG2 cells. (**B**) Images of Bcl-2-positive HepG2 cells. (**C**) Statistical analysis of Bcl-2 expression in HepG2 and Bel-7402 cells. Black arrows represent the Bcl-2-positive HepG2 and Bel-7402 cells. ** $p<0.01$, * $p<0.05$ vs. HepG2 or Bel-7402 group, # $p<0.01$ vs. 25 µg/ml RosA+0.4 µg/ml ADM group, & $p<0.01$ vs. 50 µg/ml RosA+0.4 µg/ml ADM group.

RosA combined with ADM increased Bax expression in HepG2 and Bel-7402 cells

The pre-apoptotic biomarker, Bax, was also examined using immunohistochemistry assay in HepG2 (Figure 7A) and Bel-7402 (Figure 7B) cells. The results showed that Bax expression in the RosA combined with ADM treatment group was significantly increased compared to the HepG2 group and Bel-7402 group (Figure 7C, $p<0.05$). Furthermore, Bax expression increased with increased concentration of RosA (Figure 7, $p<0.05$), which illustrates the dose-dependent difference in Bax expression among different treatment groups.

Discussion

Previous studies reported that RosA and ADM induce cell death. RosA has protective effects against liver injury and liver fibrosis by triggering its anti-apoptotic properties [19,20]. ADM usually induces apoptosis of cells through regulating the transcriptional processes [17]. However, the anti-tumor biological activities of RosA and ADM have been rarely reported in hepatic carcinoma. In recent years, there has been a growing focus on exploration of mechanisms involved in hepatic carcinoma and associated targeting of potential drugs [21]. In the present study, the anti-tumor effects of RosA and ADM and the associated mechanisms were investigated in hepatic carcinoma cell lines HepG2 and Bel-7402. Actually, our pre-experimental data showed that RosA alone and ADM alone reduce cell proliferation and
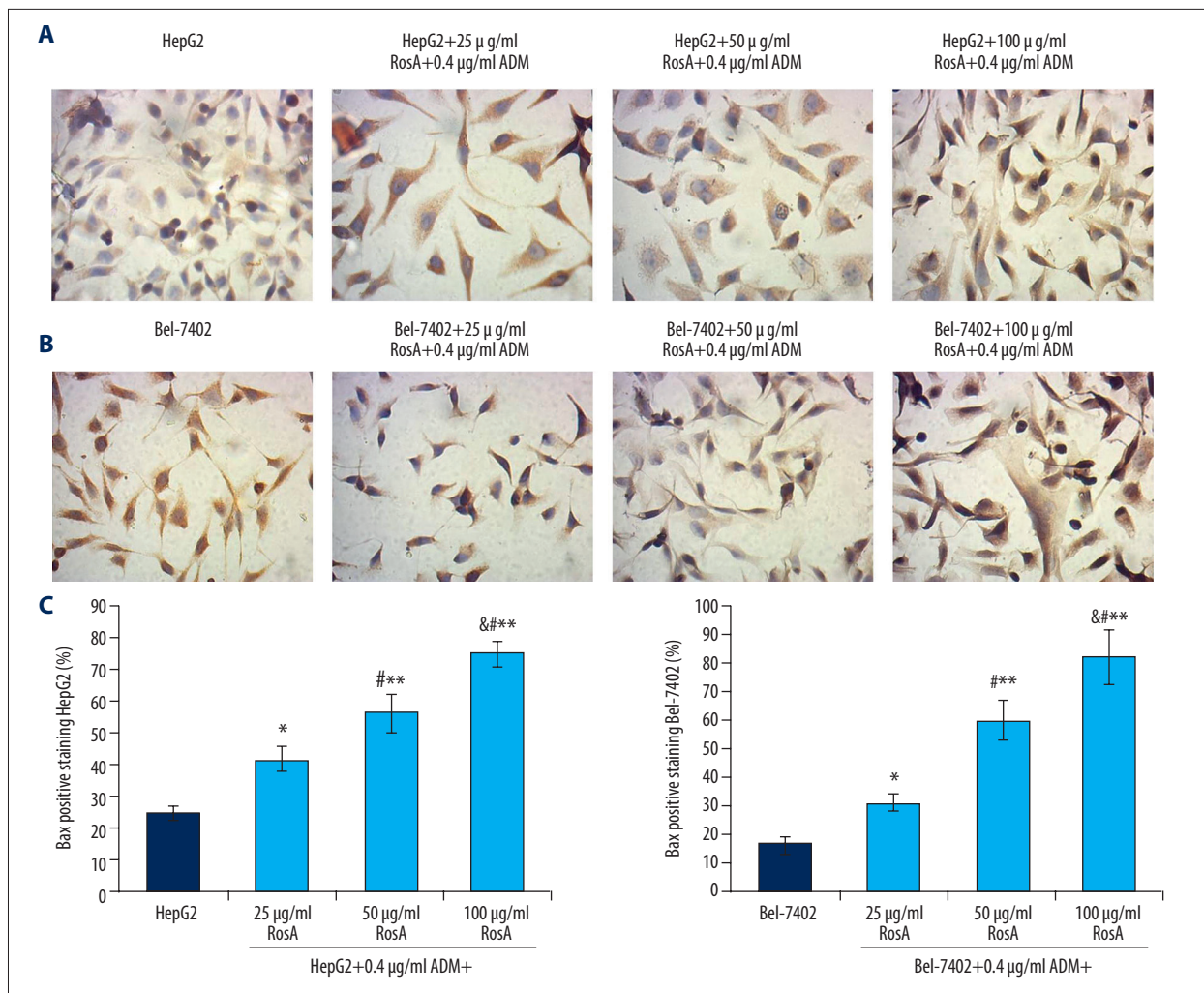
Figure 7. Evaluation of Bax expression in HepG2 and Bel-7402 cells using immunohistochemistry assay. (**A**) Images for the Bax-positive HepG2 cells. (**B**) Images for the Bax-positive HepG2 cells. (**C**) Statistical analysis for the Bax expression in HepG2 and Bel-7402 cells. Black arrows represent Bax-positive HepG2 cells. ** $p<0.01$, * $p<0.05$ *vs.* HepG2 or Bel-7402 group, # $p<0.01$ *vs.* 25 μg/ml RosA+0.4 μg/ml ADM group, & $p<0.01$ *vs.* 50 μg/ml RosA+0.4 μg/ml ADM group.

apoptosis (data not shown); therefore, in the present study we clarified the effects of RosA combined with ADM on apoptosis.

Our results showed that the morphologies of HepG2 and Bel-7402 cells were obviously damaged by treatment using RosA combined with ADM. Meanwhile, the CCK-8 assay results indicated that 25/50/100 μg/ml RosA+0.4 μg/ml ADM treatment significantly decreased cell viability compared to HepG2 and Bel-7402 cells. These results are consistent with previously published studies [22,23] showing the anti-proliferative roles of RosA and ADM. Therefore, we investigated the mechanism by which RosA and ADM cause death of HepG2 and Bel-7402 cells.

The cell cycle assay results indicated that RosA combined with ADM treatment significantly decreased G2 phase proportion and increased G1 phase proportion compared to HepG2 alone

and Bel-7402 alone. RosA combined with ADM significantly decreased the S-phase proportion in Bel-7402 cells but increased the S-phase cells in HepG2 cells, which suggests that RosA combined with ADM regulates S-phage distribution by different mechanisms in HepG2 *vs.* Bel-7402 cells, but this needs further investigation. Actually, the S-phase of the cell cycle is associated with cell apoptosis in the development of cells [24]; therefore, we speculated that RosA combined with ADM induces apoptosis of HeaG2 and Bel-7402 cells. The flow cytometry results illustrated that the apoptosis rates in the RosA (different concentrations) combined with ADM group were significantly increased compared to HepG2 alone and Bel-7402 alone. In the present study, we analyzed the apoptosis rates by calculating early apoptosis plus late apoptosis, both of which can reflect the different stages of cell apoptosis [25]. Furthermore, TUNEL was also used to evaluate DNA damage in HepG2 and

Bel-7402 cells. RosA combined with ADM significantly induced DNA damage in HepG2 and Bel-7402 cells compared to the untreated cells. DNA damage is commonly considered as an index for cell apoptosis [26]; therefore, the TUNEL results also exhibited the apoptotic functions of RosA and ADM.

Based on the effects we found using RosA combined with ADM on HepG2 and Bel-7402 cell apoptosis, the potential mechanism was also investigated in this study. Previous studies [27] reported that Bcl-2 and Bax are specific biomarkers of apoptosis for the mitochondria-associated signaling pathway. Our results indicated that RosA+ADM treatment significantly decreased Bcl-2 expression and significantly increased Bax expression compared to the HepG2 and Bel-7402 group, respectively. Bcl-2 was decreased and Bax was increased with increased concentration of RosA. Therefore, the results suggest that

RosA combined with ADM induces apoptosis of HepG2 and Bel-7402 cells by activating the mitochondria-mediated apoptosis signaling pathway.
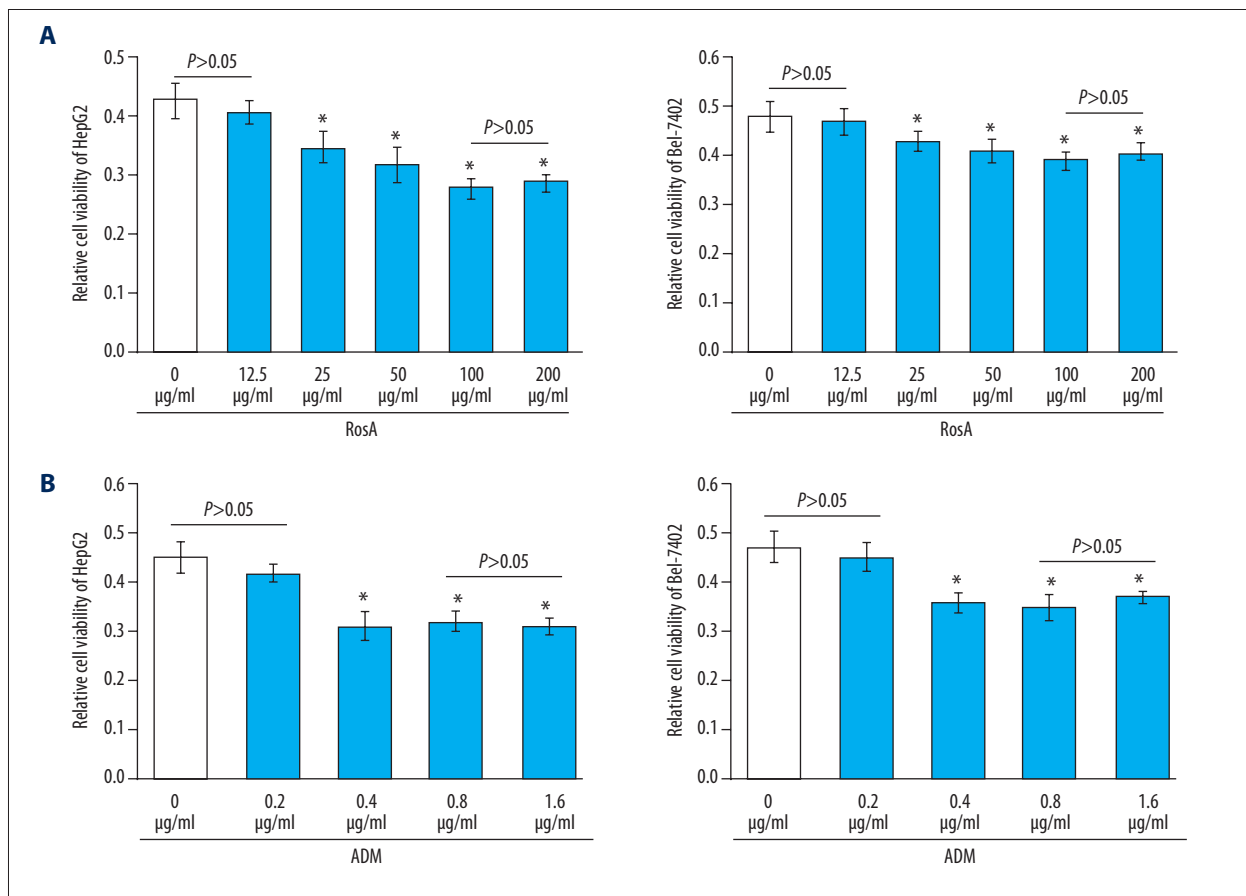
Conclusions

RosA combined with ADM damaged cell morphologies, decreased cell viability, and induced apoptosis of HepG2 and Bel-7402 cells by triggering the mitochondria-mediated signaling pathway.

Conflict of interest

None.

Supplementary Figure

Supplementary Figure 1. Cell viabilities for HepG2 and Bel-7402 cells undergoing RosA or ADM treatment, respectively. (**A**) Cell viabilities of HepG2 and Bel-7402 cells treated with different concentrations of RosA. (**B**) Cell viabilities of HepG2 and Bel-7402 cells treated with different concentrations of ADM. * $p < 0.05$ *vs.* 0 µg/ml RosA or ADM.

References:

1. Pan X, Li X, Cui L et al: Preoperative phenacetin metabolism test in the prediction of postoperative liver dysfunction of patients with hepatocellular carcinoma. Med Sci Monit, 2017; 23: 2607–11

2. Tsim NC, Frampton AE, Habib NA et al: Surgical treatment for liver cancer. World J Gastroenterol, 2010; 16: 927–33

3. Edwards BK, Ward E, Kohler BA et al: Annual report to the nation on the status of cancer, 1975-2006, featuring colorectal cancer trends and impact of interventions (risk factors, screening, and treatment) to reduce future rates. Cancer, 2010; 116: 544–73

4. Greene CM, Varley RB, Lawless MW: MicroRNAs and liver cancer associated with iron overload: Therapeutic targets unravelled. World J Gastroenterol, 2013; 19: 5212–26

5. Sun D, Qin L, Xu Y et al: Influence of adriamycin on changes in Nanog, Oct-4, Sox2, ARID1 and Wnt5b expression in liver cancer stem cells. World J Gastroenterol, 2014; 20: 6974–80

6. Villanueva A, Llovet JM: Targeted therapies for hepatocellular carcinoma. Gastroenterology 2011; 140: 1410–26

7. Asghar U, Meyer T: Are there opportunities for chemotherapy in the treatment of hepatocellular cancer? J Hepatol, 2012; 56: 686–95

8. Zhao X, Chen Q, Liu W et al: Codelivery of doxorubicin and curcumin with lipid nanoparticles results in improved efficacy of chemotherapy in liver cancer. Int J Nanomed, 2014; 10: 257–70

9. Saraswathy M, Gong S: Different strategies to overcome multidrug resistance in cancer. Biotechnol Adv, 2013; 31: 1397–407

10. Greco F, Vicent MJ: Combination therapy: Opportunities and challenges for polymer-drug conjugates as anticancer nanomedicines. Adv Drug Deliv Rev, 2009; 61: 1203–13

11. Cao W, Hu C, Wu L et al: Rosmarinic acid inhibits inflammation and angiogenesis of hepatocellular carcinoma by suppression of NF-κB signaling in H22 tumor-bearing mice. J Pharmacol Sci, 2016; 132: 131–37

12. Osakabe N, Yasuda A, Natsume M et al: Rosmarinic acid inhibits epidermal inflammatory responses: Anticarcinogenic effect of perilla frutescens extract in the murine two-stage skin model. Carcinogenesis, 2004; 25: 549–57

13. Han S, Yang S, Cai Z et al: Anti-Warburg effect of rosmarinic acid via miR-155 in gastric cancer cells. Drug Des Devel Ther, 2015; 9: 2695–703

14. Moon DO, Kim MO, Lee JD et al: Rosmarinic acid sensitizes cell death through suppression of TNF-alpha-induced NF-κB activation and ROS generation in human leukemia U937 cells. Cancer Lett, 2010; 288: 183–91

15. Venkatachalam K, Gunasekaran S, Jesudoss VA et al: The effect of rosmarinic acid on 1,2-dimethylhydrazine induced colon carcinogenesis. Exp Toxicol Pathol, 2013; 65: 409–18

16. Yao H, Cai ZY, Sheng ZX: NAC attenuates adriamycin-induced nephrotic syndrome in rats through regulating TLR4 signaling pathway. Eur Rev Med Pharmacol Sci, 2017; 21: 1938–43

17. Bessone F: Non-steroidal anti-inflammatory drugs: What is the actual risk of liver damage? World J Gastroenterol, 2010; 16: 5651–61

18. Han HJ, Kwon HY, Sohn EJ et al: Suppression of E-cadherin mediates gallotannin induced apoptosis in HepG2 hepatocellular carcinoma cells. Int J Biol Sci, 2014; 10: 490–99

19. Domitrovic R, Skoda M, Vasiljev Marchesi V et al: Rosmarinic acid ameliorates acute liver damage and fibrogenesis in carbon tetrachloride-intoxicated mice. Food Chem Toxicol, 2013; 51: 370–78

20. Yang MD, Chiang YM, Higshiyama R et al: Rosmarinic acid and baicalin epigenetically derepress peroxisomal proliferator-activated receptor gamma in hepatic stellate cells for their anti-fibrotic effect. Hepatology, 2012; 55: 1271–81

21. Zhao XQ, Liang B, Jiang K et al: Down-regulation of miR-655-3p predicts worse clinical outcome in patients suffering from hepatocellular carcinoma. Eur Rev Med Pharmacol Sci, 2017; 21: 748–52

22. Yan F, Bai LP, Gao H et al: EGF reverses multi-drug resistance via p-ERK pathway in HepG2/ADM and SMMC7721/ADM hepatocellular carcinoma models. Asian Pac J Cancer Prev, 2014; 15: 2619–23

23. Wu J, Zhu Y, Li F et al: Spica prunellae and its marker compound rosmarinic acid induced the expression of efflux transporters though activation of Nrf2-mediated signaling pathway in HepG2 cells. J Ethnopharmacol, 2016; 193: 1–11

24. Liu D, Yang Y, Liu Q et al: Inhibition of autophagy by 3-MA potentiates cisplatin-induced apoptosis in esophageal squamous cell carcinoma cells. Med Oncol, 2011; 28: 105–11

25. Hu Z, Zhang H, Tang L et al: Silencing nc886, a non-coding RNA, induces apoptosis of human endometrial cancer cells-1A in vitro. Med Sci Monit, 2017; 23: 1317–24

26. Zheng H, Wang S, Zhou P et al: Effects of ligustrazine on DNA damage and apoptosis induced irradiation. Environ Toxicol Pharamacol, 2013; 36: 1197–206

27. Wang N, Wang W, Huo P et al: Mitochondria-mediated apoptosis inhuman lung cancer A549 cells by 4-methylsulfinyl-3-butenyl isothiocyanate from radish seeds. Asian Pac J Cancer Prev, 2014; 15: 2133–39